Z. Kristallogr. Suppl. **26** (2007) 345-350

Microstructure evolution of nanocrystalline HITPERM and NANOPERM alloys: Insight from *in-situ* synchrotron radiation experiments

R. Nicula[1,*], V.D. Cojocaru[2], J. Bednarcik[1,3], M. Stir[1] and E. Burkel[1]

[1]Institute of Physics, Rostock University, August-Bebel-Str. 55, 18055 Rostock, Germany
[2]University POLITEHNICA Bucharest, Spl. Independentei 313, 77206 Bucharest, Romania
[3]Institute of Physics, P.J. Safarik University, Park Angelinum 9, 04154 Košice, Slovakia
[*] Contact author; e-mail: nicula@physik1.uni-rostock.de

Keywords: *in-situ* powder diffraction, grain-growth kinetics, magnetic nanocomposites

Abstract. The properties of nanocrystalline materials differ from the ones of their coarse-grained counterparts. Significant changes of the phase diagrams were also recently reported for various nanomaterials. Thermomechanical processing routes - with or without pressure application - employed to obtain bulk nanostructured solids from nanocrystalline powders control the microstructural features down to the nanoscale and thus determine the final nanomaterial properties. Modern *in-situ* X-ray diffraction experiments provide effective tools for the observation and engineering of the microstructure in nanomaterials. Time-resolved *in-situ* synchrotron radiation diffraction experiments were here used to monitor the evolution of the weighted column-length distributions and microstrain at specimen-relevant scales during heating of nanocrystalline HITPERM and NANOPERM alloys. Diffraction line profile analysis methods were applied to observe the grain growth kinetics in these Fe(Co)-Zr-B-Cu nanostructured alloys. The retention of their excellent soft magnetic properties in particular at high temperature depends on the ability to supress anomalous grain growth.

Introduction

High-performance magnets operating at high temperatures are essential to important modern applications, e.g. space power generation systems, transformers and magnetomechanical actuators [1]. These applications require novel soft magnetic materials with high remanence and saturation magnetization, low coercivity, low hysteretic and eddy-current losses and high Curie temperatures, together with improved mechanical properties and corrosion resistance. Amorphous and nanocrystalline Fe–Co alloys were developed to meet these requirements [1–3]. The potential of nanostructured alloys as modern soft magnetic materials relies on the fact that for crystallite dimensions below a critical size, the coercivity H_c decreases rapidly

with decreasing grain size, as predicted by Herzer's random anisotropy model [4]. However, a major challenge remains the identification of powder processing routes able to retain ultra-fine microstructures and the exchange coupling between the magnetic nanoparticles within bulk nanostructured magnets operating at elevated temperatures [1]. The need for large magnetic inductions and Curie temperatures imposes strong restrictions on the choice of soft magnetic alloys for high-temperature applications, limited in essence to Fe–Co alloys. For binary Fe–Co alloys, the peak of the Slater–Pauling curve is attained at compositions close to 30% Co [5], while other properties of interest rather favour the equiatomic composition.

Time-resolved *in-situ* synchrotron radiation diffraction was used to monitor the evolution of alloy microstructure at specimen-relevant scales during heating of nanocrystalline HITPERM and NANOPERM alloys. Line profile analysis [6] was applied to investigate the kinetics of microstructure coarsening in these Fe(Co)-Zr-B-Cu alloys.

Experimental

Nanocrystalline alloys with nominal compositions (at.%) $Fe_{88}Zr_7B_4Cu_1$ (NANOPERM) and $Fe_{44}Co_{44}Zr_7B_4Cu_1$ (HITPERM) were prepared from high purity (> 99.8 %, Mateck GmbH) constitutive elements by mechanical alloying (planetary ball-mill RETSCH PM 400). The powder mixtures were wet-milled in hexane for 90 hours, using stainless steel vial and balls (ball-to-powder mass ratio 18:1, wheel speed 250 rpm). The temperature-resolved structural and microstructure evolution of the mechanically-alloyed HITPERM and NANOPERM specimens during non-isothermal heating was investigated by *in-situ* angular-dispersive X-ray diffraction at the high-resolution powder diffractometer at the B2 beamline (HASYLAB DESY, Hamburg, Germany). The synchrotron radiation wavelength was set to $\lambda = 0.7095$ Å. The heating experiments were performed using an OBI image plate detector and a STOE furnace [7]. Electron microscopy analysis of the specimens morphology and chemical composition was performed using a ZEISS DSM 960A electron microscope.

Results and discussion

The high-energy wet-milling of the as-received high-purity elemental powders results in the desired NANOPERM and HITPERM alloys after 90 hours. The progress of the mechanical alloying process was monitored by X-ray diffraction and SEM analysis at different stages of processing. Lamellar aggregates were still evidenced up to 80 hours wet-milling, indicating that the alloying process was not completed, in spite of the rather long ball-milling times. Wet milling in hexane was used to efficiently avoid oxidation of the powders, and to strongly reduce adhesion to and contamination (mostly iron or chromium) from the stainless steel milling equipment, thus avoiding undesired deviations from the target chemical composition. The typical morphology of the alloy powders after 90 hours wet-milling is shown in Fig. 1 (NANOPERM) and Fig. 2 (HITPERM). The average powder particle size is about 10 µm for both alloys, however the Co-containing HITPERM alloys show a more pronounced polydispersity, i.e. powder particles of only 1-2 µm diameter coexist with much larger ones, of up to 20 µm in size. Most powder particles have a flattened morphology typical for materials processed by ball-milling with smooth surfaces.

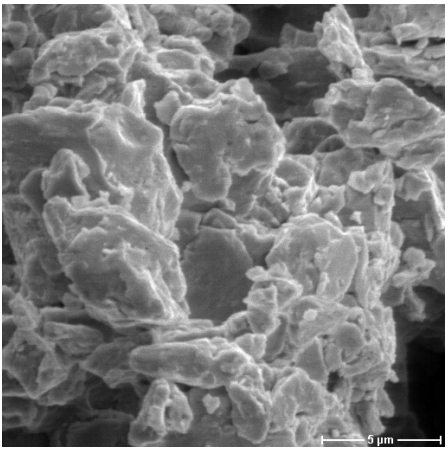

Figure 1. Scanning electron microscopy (SEM) micrograph of as-prepared NANOPERM alloy nanopowders (wet-milled for 90 hours).

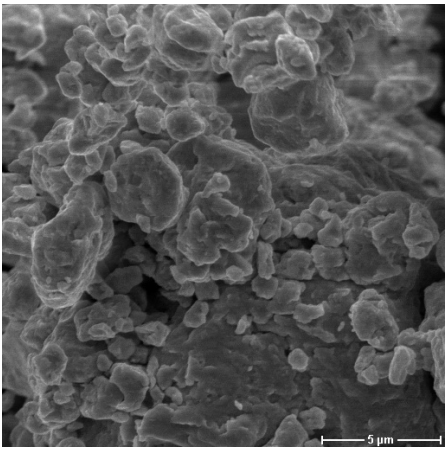

Figure 2. SEM micrograph showing the typical morphology of HITPERM alloy nanopowders.

The synchrotron radiation diffraction patterns collected *in-situ* during the non-isothermal heating of the NANOPERM alloy powders are shown as 2D X-ray intensity map in Figure 3. In the as-milled state, the Fe-Zr-B-Cu powders consist of solid solution with a bcc structure. The bcc α to fcc γ transition is also observed at temperatures above 800°C.

The full-pattern decomposition of the X-ray diffraction patterns was performed with the PEAKFIT© software package [8] using Voigt profiles. The (110) and (220) diffraction lines of the bcc-(Fe,Co) nanocrystalline phase were used to infer the volume-weighted domain size and r.m.s. strain (Fig. 4).

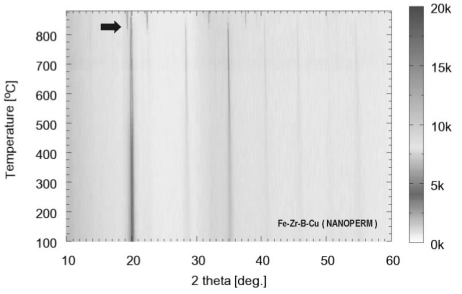

Figure 3. Synchrotron radiation powder diffraction patterns collected during constant rate heating of NANOPERM powders ball-milled for 90 hours.

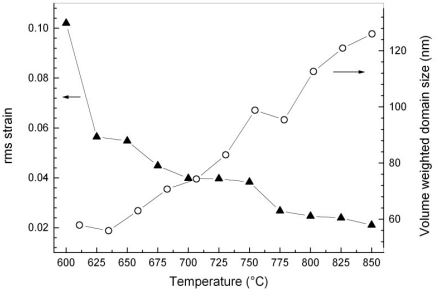

Figure 4. Temperature evolution of the volume-weighted domain size and rms strain for the bcc-(Fe,Co) main phase of the HITPERM alloy.

The double-Voigt line-profile analysis method [6] was used to obtain the volume-weighted column-length distribution functions $p_V(L)$ at different temperatures. The column-length

distributions $p_V(L)$ were least-squares fitted to log-normal and gamma distribution functions. The column-length distributions are better described by gamma functions (Fig. 5).

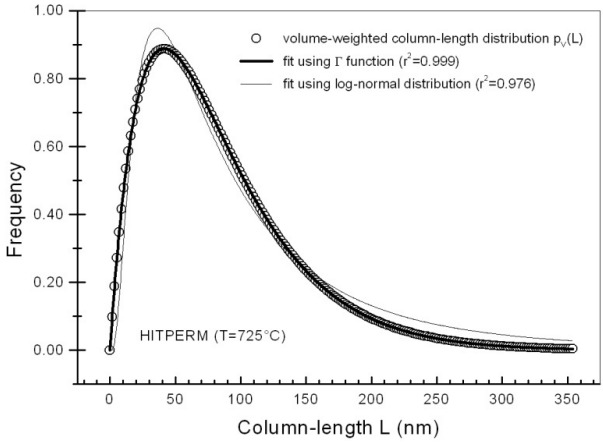

Figure 5. Comparison between the results of least-squares fitting of the volume-weighted column length $p_V(L)$ distribution (open squares) of NANOPERM using a gamma function (thick line) and a log-normal distribution (thin line).

The area-normalized gamma function distributions resulting from the least-squares fitting of the $p_V(L)$ distributions are shown in Fig. 6 (NANOPERM) and Fig. 7 (HITPERM).

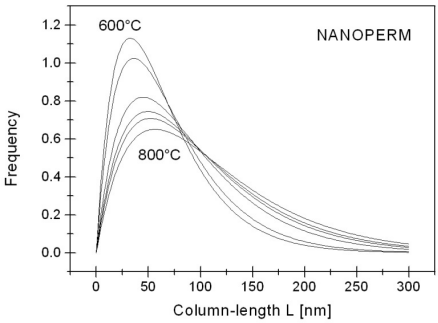

Figure 6. Temperature-resolved evolution of the volume-weighted column-length distribution of NANOPERM alloys during heating.

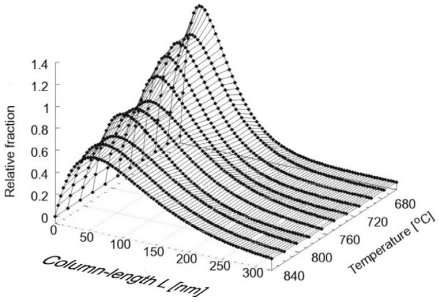

Figure 7. Temperature evolution of the volume-weighted column-length distribution (HITPERM).

In order to retrieve grain-size distributions g(D) from the column-length distributions p(L), further corrections must be applied. One necesarily assumes that certain conditions are met, i.e. most grains have approximatively the same shape (e.g spherical), no or moderate strains

are present and the analytical form of the grain-size distribution (e.g. log-normal) is a priori known and valid at all temperatures [9]. The validity of these assumptions is questionable for high-energy ball-milled powders [9], so that a further quantitative analysis would eventually yield doubtful results. On the other hand, the grain-size distribution g(D) is solely determined by the distribution of column-lengths p(L) [9,10]. Therefore, as long as the shape of the crystallites is preserved, one may expect that changes induced by either isothermal or non-isothermal thermal treatments are reflected by both p(L) and g(D) distributions in a similar manner. This concerns not only the average scale of the microstructure but also the actual degree of microstructural homogeneity. Our *in-situ* synchrotron radiation experiments clearly evidence the increase of the average grain size with temperature, but also the widening of the size distribution, which may further be monitored via its variance. This additional - often not exploited - information allows for the earlier detection of anomalous grain growth events and provide considerable insight into the sinterability and the kinetics of sintering processes for nanocrystalline powders at different temperatures [11].

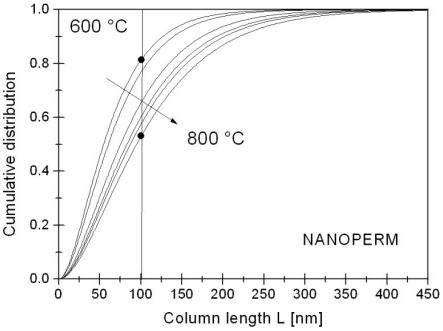

Figure 8. Temperature evolution of the cumulative distribution of column lengths (NANOPERM).

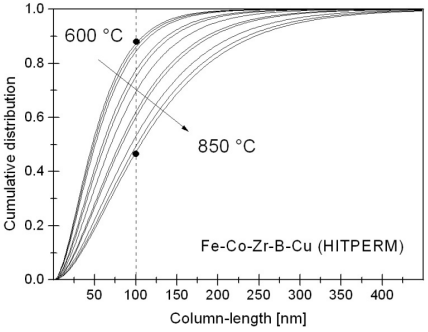

Figure 9. Temperature evolution of the cumulative distribution of column lengths(HITPERM alloys).

Temperature-resolved cumulative distributions were as well derived (Fig. 8 and 9) from the column-length $p_V(L)$ distributions, yielding the fraction of columns having lengths below a certain arbitrary value. For the NANOPERM powders, one may readily conclude that while at 600°C about 82 % of the columns are less than 100 nm in length, this fraction drops down to only 49 % at 800°C (Fig. 8). For the HITPERM alloy, we estimate the fraction of columns with lengths below 100 nm to reach 84% at 600°C and only 43% at 850°C (Fig. 9).

Concluding remarks

The temperature- and time-dependence of the alloy microstructure may be followed in detail via the evolution of weighted column-length distributions. Grain-size distributions may also be retrieved under certain circumstances. *In-situ* synchrotron radiation X-ray diffraction experiments provide an accurate statistical description of the temperature- / time-dependent evolution of the microstructure. In particular, the information contained in the shape and width (variance) of the size distributions is essential to the guidance of sintering experiments.

Preliminary results based on *in-situ* synchrotron radiation diffraction experiments were here obtained on the microstructural evolution of nanocrystalline HITPERM and NANOPERM Fe(Co)-Zr-B-Cu alloys for the high-temperature interval between 600-850°C.

References

1. McHenry, M.E., Willard, M.A. & Laughlin, D.E., 1999, *Prog. Mater. Sci.*, **44**, 291.
2. Willard, M.A., Laughlin, D.E. & McHenry, M.E., 2000, *J. Appl. Phys.*, **87**, 7091.
3. McHenry, M.E. & Laughlin, D.E., 2000, *Acta Mater.*, **48**, 223.
4. Herzer, G. in Idzikowski, B., Svec, P. & Miglierini, M. (Eds.), 2005, *Properties and Applications of Nanocrystalline Alloys from Amorphous Precursors* (Kluwer Academic Publishers), pp. 15–34 and references therein.
5. McLaren, J.M., Schulthess, T.C., Butler, W.H., Sutton, R. & McHenry, M., 1999, *J. Appl. Phys.*, **85**, 4833.
6. Balzar, D. & Ledbetter, H., 1993, *J. Appl. Cryst.*, **26**, 97.
7. Knapp, M., Baehtz, C., Ehrenberg, H. & Fuess, H., 2004, *J. Synch. Rad.*, **11**, 328.
8. PeakFit for Windows User's Manual, SPSS Science, Inc., ISBN 1-56827-183-2.
9. Krill, C.E. & Birringer, R., 1998, *Phil. Mag.*, **77**, 621.
10. Smith, W.L., 1976, *J. Appl. Cryst.*, **9**, 187.
11. Chappell, J.S., Ring, T.A. & Birchall, J.D., 1986, *J. Appl. Phys.*, **60**, 383.

Acknowledgements. We acknowledge Dr. M. Knapp and Dr. C. Baehtz for the friendly help at the B2 beamline in HASYLAB/DESY. This work was financially supported by the Marie Curie Programme of the European Community (HPMD-CT-2001-00089).